Fine structure of the nucleon electromagnetic form factors in the vicinity of the threshold of e+e- annihilation into nucleon - antinucleon pair

A.I. Milstein

G.I.Budker Institute of Nuclear Physics, Novosibirsk, Russia

Layout

- Close to the threshold of $N\bar{N}$, but not very close:
  $e^+e^- \to p\bar{p}$, $n\bar{n}$, mesons; $J/\psi \to p\bar{p}\pi^0(\eta)$; $J/\psi \to p\bar{p}\rho(\omega)$;
  J/ψ, $\psi(2S) \to p\bar{p}\gamma$; $J/\psi \to \gamma\eta'\pi^+\pi^-$ decay.
- Very close to the threshold of $N\bar{N}$:
  Approach of calculation of σ_{el} ($e^+e^- \to p\bar{p}$ and $e^+e^- \to n\bar{n}$),
  σ_{in} ($e^+e^- \to$ mesons), and σ_{tot} cross sections.
- Our predictions for σ_{el}, σ_{in}, and σ_{tot} cross sections. Discussion of isospin-violating effects.
- Conclusion

$e^+e^- \to p\bar{p}$, near the threshold of the process, strong energy dependence!

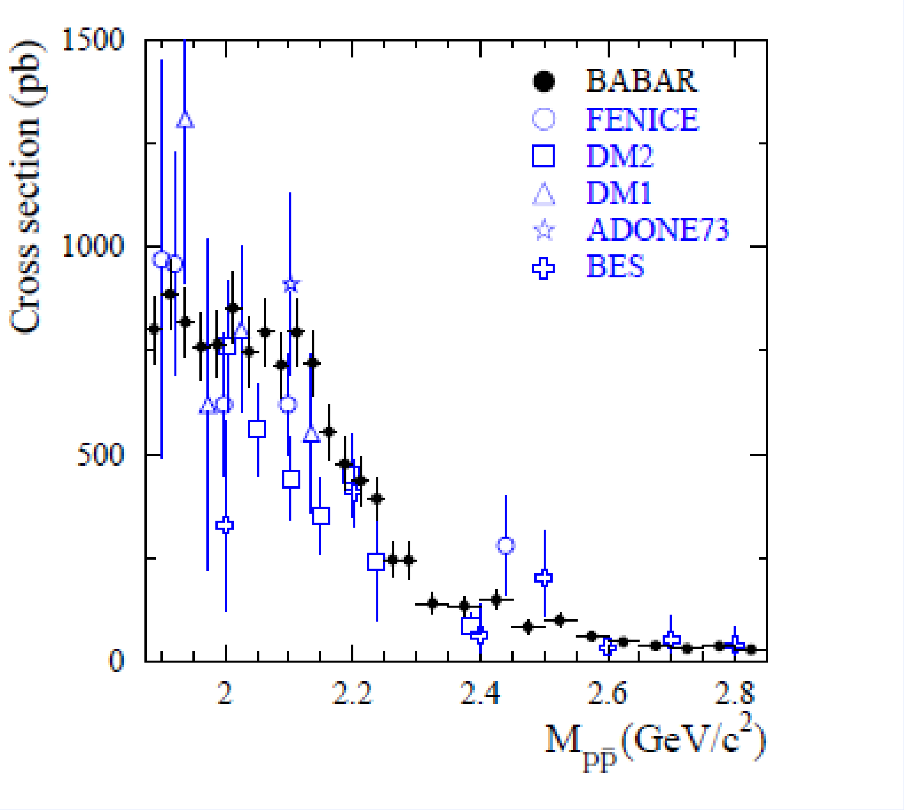

Cross section $e^+e^- \to p\bar{p}$; data are from B. Aubert, et al., BaBar, Phys. Rev. D 73, 012005 (2006)

$e^+e^- \to n\bar{n}$, $3(\pi^+\pi^-)$ near the threshold of $N\bar{N}$ pair production

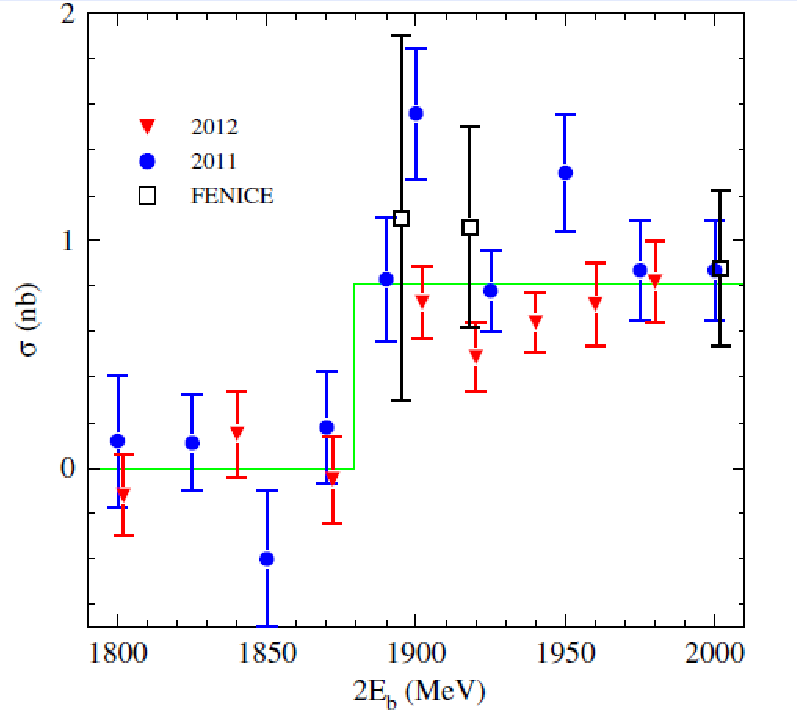

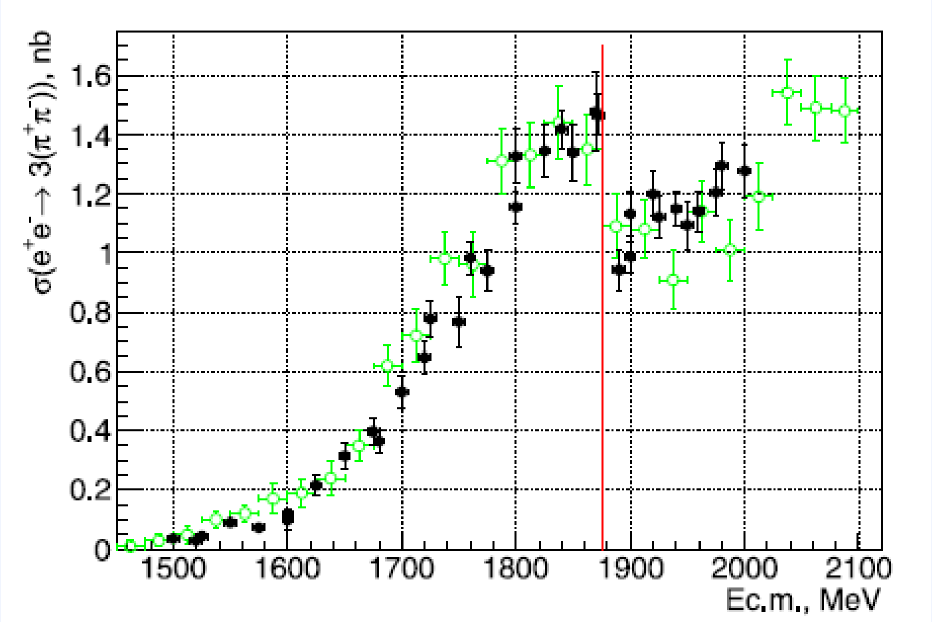

Left picture: cross section $e^+e^- \to n\bar{n}$; data are from M.N. Achasov, et al., SND, Phys. Rev. D 90, 112007 (2014); right picture: cross section $e^+e^- \to 3(\pi^+\pi^-)$; data are from R.R.Akhmetshin, et al., CMD3,Physics Letters, B723, 634 (2013),(black dots); B. Aubert, et al., BaBar , Phys. Rev. D 73 (2006) 052003, (green open circles)

$$e^+e^- \to 2(\pi^+\pi^-\pi^0)$$

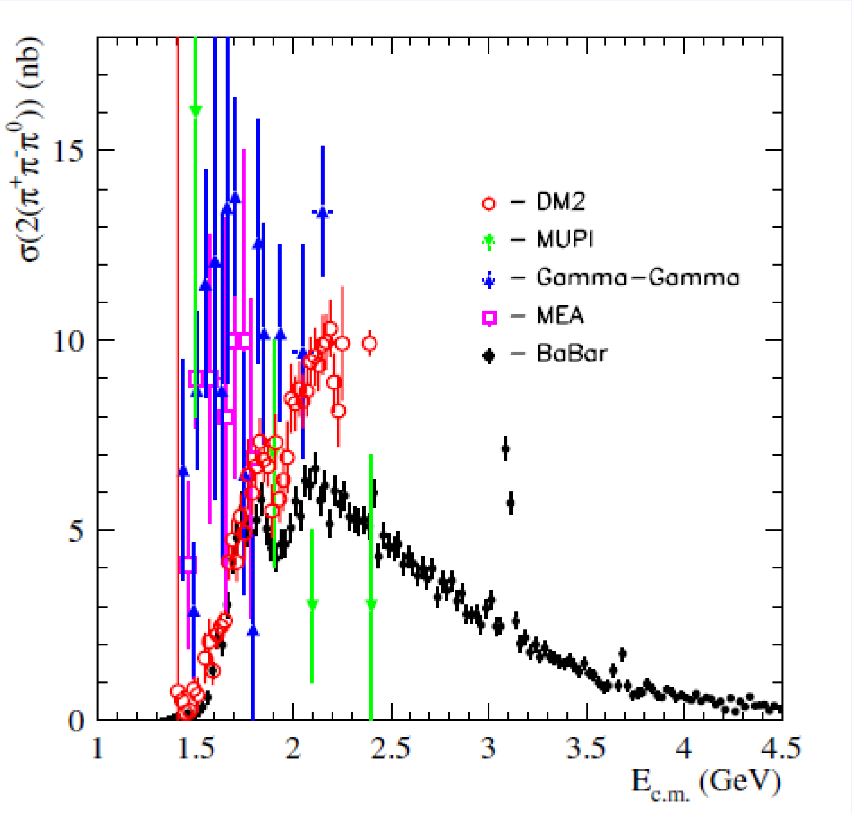

Cross section $e^+e^- \to 2(\pi^+\pi^-\pi^0)$; from B. Aubert, et al., BaBar , Phys. Rev. D 73 (2006) 052003

Strong enhancement of decay probability at low invariant mass of $p\bar{p}$ in the processes $J/\Psi \to \gamma p\bar{p}$, $B^+ \to K^+ p\bar{p}$ and $B^0 \to D^0 p\bar{p}$, $B^+ \to \pi^+ p\bar{p}$ and $B^+ \to K^0 p\bar{p}$, $\Upsilon \to \gamma p\bar{p}$... These effects are similar to that in e^+e^- annihilation.

One of the most natural explanation of this enhancement is final state interaction of nucleon and antinucleon

B. Kerbikov, A. Stavinsky, and V. Fedotov, Phys. Rev. C **69**, 055205 (2004); D.V. Bugg, Phys. Lett. B **598**, 8 (2004); B. S. Zou and H. C. Chiang, Phys. Rev. D **69**, 034004 (2004); B. Loiseau and S. Wycech, Phys. Rev. C **72**, 011001 (2005); A. Sibirtsev, J. Haidenbauer, S. Krewald, Ulf-G. Meiner, and A.W. Thomas, Phys. Rev. D **71**, 054010 (2005); J. Haidenbauer, Ulf-G. Meiner, A. Sibirtsev, Phys.Rev. D **74**, 017501 (2006); V.F. Dmitriev and A.I.Milstein, Phys. Lett. B 658 (2007), 13.

Final state interaction

Final state interaction (including annihilation channels) may be taken into account by means optical potentials:

$$V_{N\bar{N}} = U_{N\bar{N}} - iW_{N\bar{N}}\,.$$

Nijmegen, Paris, Jülich... optical potentials give the same predictions for the cross sections of elastic and inelastic scattering of unpolarized particles but essentially different predictions for spin observables!
The cross section $\sigma = \sigma_{ann} + \sigma_{cex} + \sigma_{el}$ of $p\bar{p}$ scattering has the form

$$\sigma = \sigma_0 + (\boldsymbol{\zeta}_1\cdot\boldsymbol{\zeta}_2)\,\sigma_1 + (\boldsymbol{\zeta}_1\cdot\boldsymbol{\nu})(\boldsymbol{\zeta}_2\cdot\boldsymbol{\nu})\,(\sigma_2-\sigma_1)\,,$$

where ζ_1 and ζ_2 are the unit polarization vectors of the proton and antiproton, respectively.
Investigation of the process $e^+e^- \to N\bar{N}$ gives important information for modification of optical potentials!

Near the threshold but not very close to the threshold.

It is possible to neglect the proton-neutron mass difference and the Coulomb potential. Our predictions for $e^+e^- \to N\bar{N}$ [V.F.Dmitriev, A.I.Milstein, S.G. Salnikov, PR D93, 034033 (2016)]

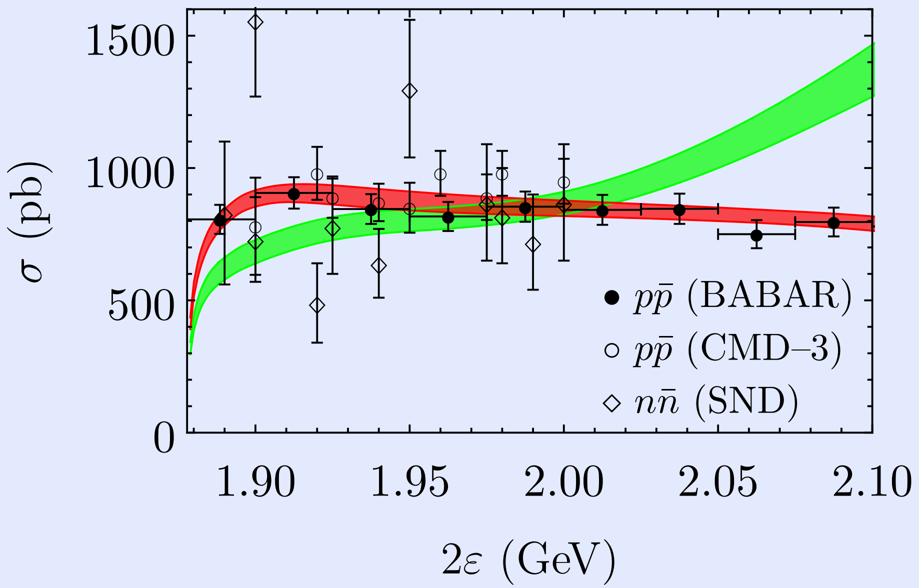

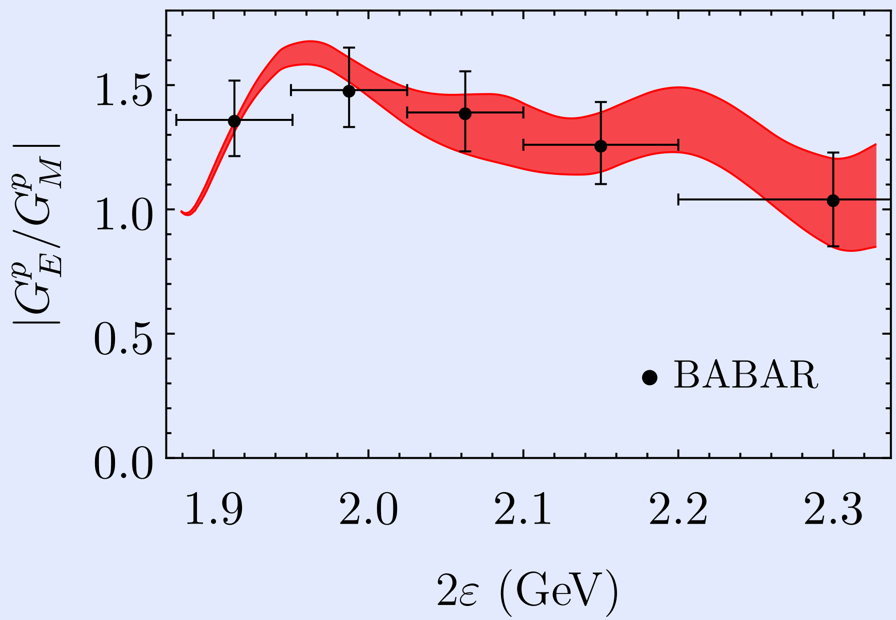

Left: the cross sections of $p\bar{p}$ (red line) and $n\bar{n}$ (green line) production, Right: $|G_E^p/G_M^p|$ for proton. The experimental data are from J.P.Lees et al., BaBar, Phys.Rev. D 87, 092005 (2013), R.R. Akhmetshin et al., CMD3, Physics Letters B759, 634 (2016) M.N. Achasov et al.,SND, Phys. Rev. D 90, 112007 (2014).

$e^+e^- \to 6\pi$ near the threshold (via virtual $N\bar{N}$ pair production).

The cross section in the energy region between 1.7 GeV and 2.1 GeV is approximated by the formula

$$\sigma_{6\pi} = A\sigma^1_{\rm ann} + B \cdot E + C,$$

where the best coincidence is for $A = 0.56$, $B = 0.012$ nb/MeV, $C = 4.96$ nb. The coefficient A agrees with the data of $p\bar{p} \to pions$ annihilation at rest, where 6π give $\sim 55\%$ of $I = 1$ contribution (C. Amsler et al., Nucl. Phys. A720, 357 (2003)).

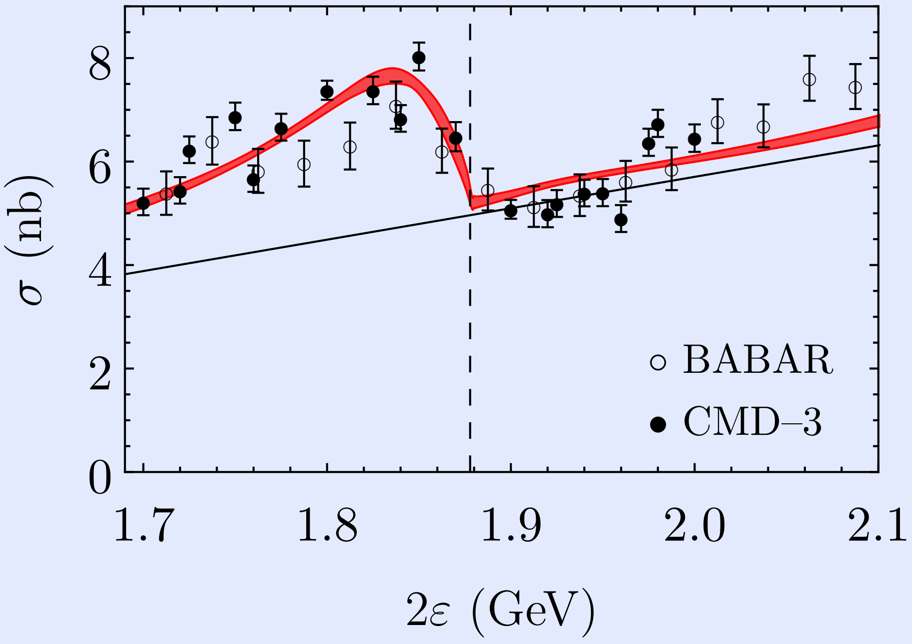

The invariant mass spectra of $J/\psi \to p\bar{p}\pi^0$ and $J/\psi \to p\bar{p}\eta$ decays [V.F.Dmitriev, A.I.Milstein, S.G. Salnikov, PL B 760, 139 (2016)]:

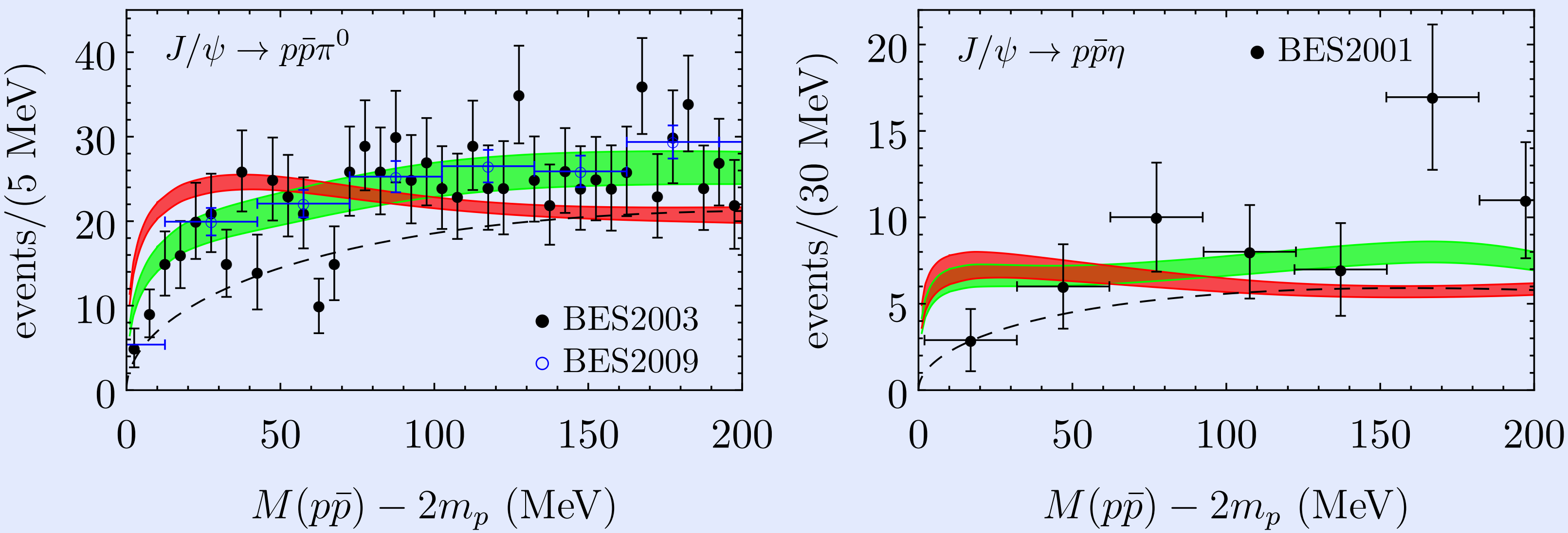

Left: $J/\psi \to p\bar{p}\pi^0$ decay. Right: $J/\psi \to p\bar{p}\eta$ decay. The red band corresponds to our previous parameters of the potential and the green band corresponds to the refitted model. The phase space behavior is shown by the dashed curve.

$J/\psi \to p\bar{p}\gamma\ (\rho\ ,\omega)$ decays

A.I.Milstein, S.G.Salnikov, Nucl. Phys. A 966, 54 (2017)

Dominant contribution is given by the state of $p\bar{p}$ pair with the quantum numbers $J^{PC} = 1^{-+}\ (^1S_0)$. The invariant mass spectra in $J/\psi \to p\bar{p}\rho\,(\omega)$ decays:

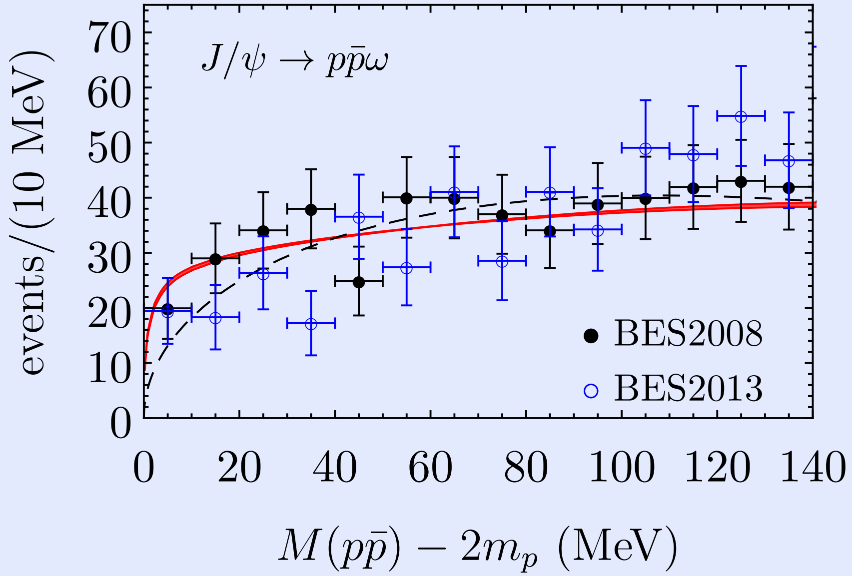

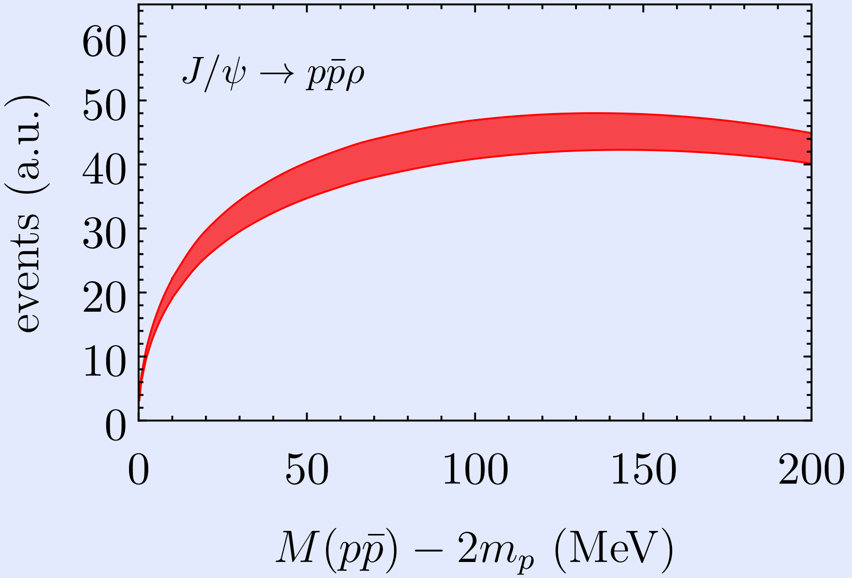

Left: $J/\psi \to p\bar{p}\omega$ decay. Right: $J/\psi \to p\bar{p}\rho$ decay.

J/ψ, $\psi(2S) \to p\bar{p}\gamma$ decay

The invariant mass spectra in $J/\psi(\psi(2S) \to p\bar{p}\gamma$ decays:

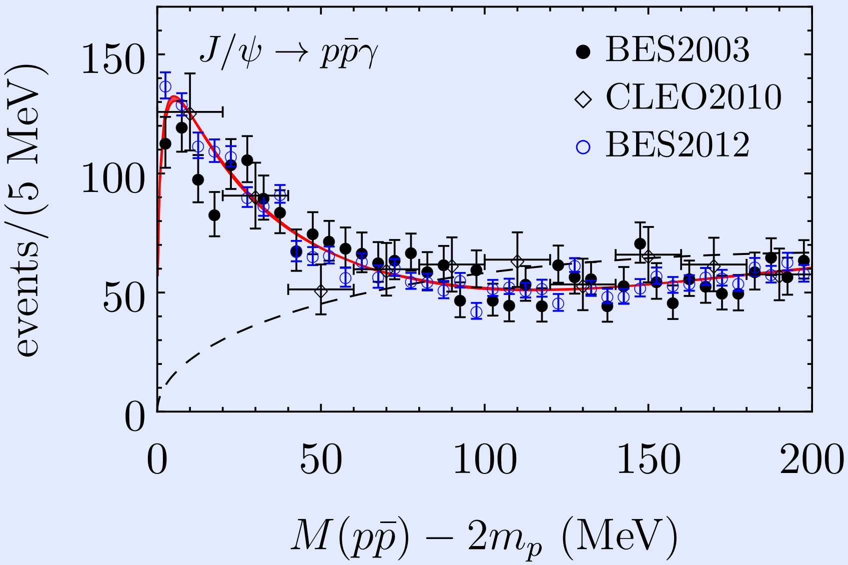

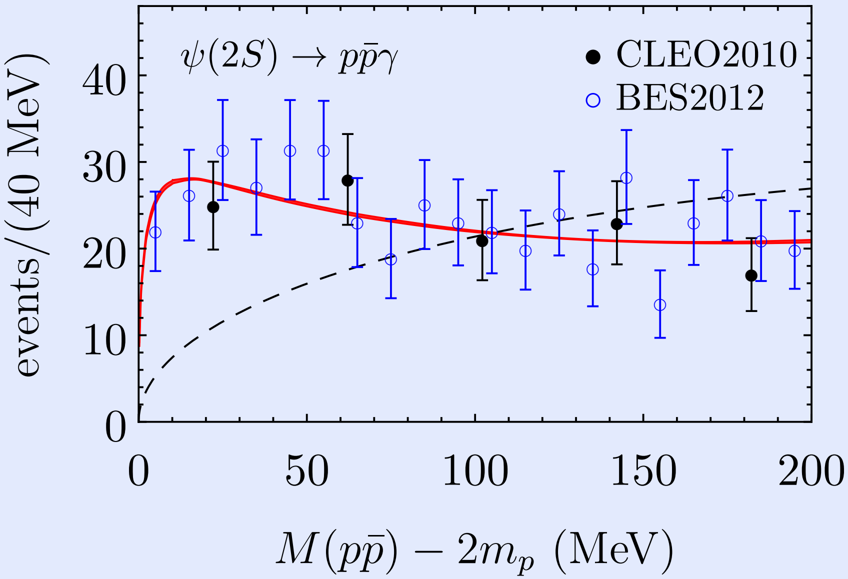

Left: $J/\psi \to p\bar{p}\gamma$ decay. Right: $\psi(2S) \to p\bar{p}\gamma$ decay.

The $\eta'\pi^+\pi^-$ invariant mass spectrum in $J/\psi\to\gamma\eta'\pi^+\pi^-$ decay:

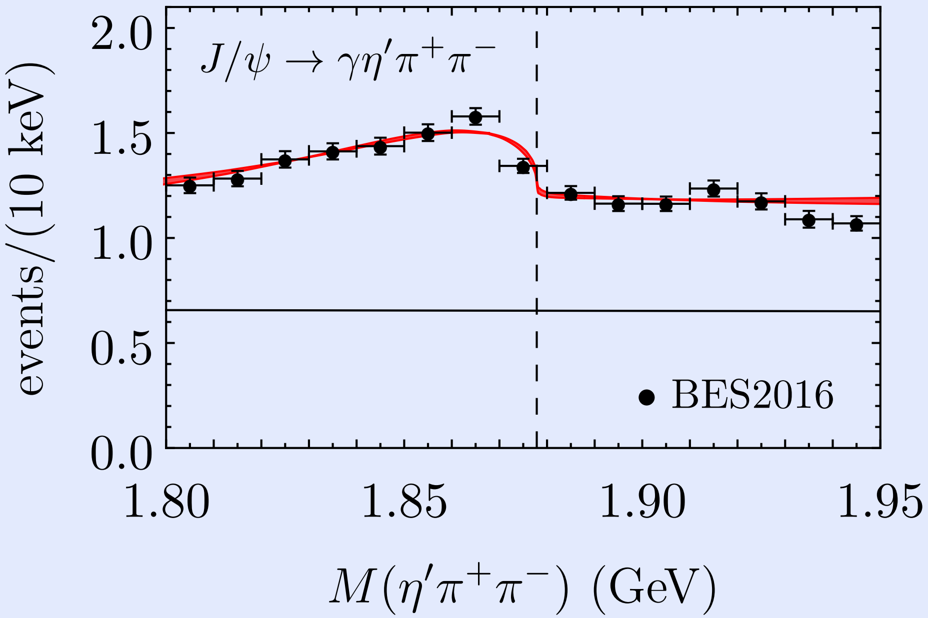

The thin line shows the contribution of non-$N\bar{N}$ channels. Vertical dashed line is the $N\bar{N}$ threshold.

Very close to the thresholds.

(A.I.Milstein, S.G.Salnikov, arXiv:1804.01283)

It is necessary to take also into account the proton-neutron mass difference and the Coulomb potential. The coupled-channels radial Schrdinger equation for the ${}^3S_1 -{}^3 D_1$ states reads

$$\left[p_r^2 + \mu\mathcal{V} - \mathcal{K}^2\right]\Psi = 0\,, \qquad \Psi^T = (u^p, w^p, u^n, w^n)\,,$$
$$\mathcal{K}^2 = \begin{pmatrix} k_p^2\mathbb{I} & 0 \\ 0 & k_n^2\mathbb{I}\end{pmatrix}, \qquad \mathbb{I} = \begin{pmatrix} 1 & 0 \\ 0 & 1\end{pmatrix}, \quad \mu = \frac{1}{2}\left(m_p + m_n\right),$$
$$k_p^2 = \mu E\,, \qquad k_n^2 = \mu(E - 2\Delta)\,, \qquad \Delta = m_n - m_p\,,$$

where $(-p_r^2)$ is the radial part of the Laplace operator, $u^p(r)$, $w^p(r)$ and $u^n(r)$, $w^n(r)$ are the radial wave functions of a proton-antiproton or neutron-antineutron pair with the orbital angular momenta $L = 0$ and $L = 2$, respectively, m_p and m_n are the proton and neutron masses, E is the energy of a system counted from the $p\bar{p}$ threshold.

The optical potential.

$\mathcal{V}$ is the matrix 4×4 which accounts for the $p\bar{p}$ interaction and $n\bar{n}$ interaction as well as a transition $p\bar{p} \leftrightarrow n\bar{n}$. This matrix can be written in a block form as

$$\mathcal{V} = \begin{pmatrix} \mathcal{V}^{pp} & \mathcal{V}^{pn} \\ \mathcal{V}^{pn} & \mathcal{V}^{nn} \end{pmatrix},$$

where the matrix elements read

$$\mathcal{V}^{pp} = \frac{1}{2}(\mathcal{U}^1 + \mathcal{U}^0) - \frac{\alpha}{r}\mathbb{I} + \mathcal{U}_{cf}\,, \qquad \mathcal{V}^{nn} = \frac{1}{2}(\mathcal{U}^1 + \mathcal{U}^0) + \mathcal{U}_{cf}\,,$$

$$\mathcal{V}^{pn} = \frac{1}{2}(\mathcal{U}^0 - \mathcal{U}^1)\,, \qquad \mathcal{U}_{cf} = \frac{6}{\mu r^2}\begin{pmatrix} 0 & 0 \\ 0 & 1 \end{pmatrix},$$

$$\mathcal{U}^I = \begin{pmatrix} V_S^I & -2\sqrt{2}\,V_T^I \\ -2\sqrt{2}\,V_T^I & V_D^I - 2V_T^I \end{pmatrix}.$$

$V_S^I(r)$, $V_D^I(r)$, and $V_T^I(r)$ are the terms in the potential V^I of the strong $N\bar{N}$ interaction, corresponding to the isospin I,

$$V^I = V_S^I(r)\delta_{L0} + V_D^I(r)\delta_{L2} + V_T^I(r)\left[6\,(\boldsymbol{S}\cdot\boldsymbol{n})^2 - 4\right].$$

Here $\boldsymbol{S}$ is the spin operator of the produced pair ($S=1$) and $\boldsymbol{n}=\boldsymbol{r}/r$. The optical potential V is expressed via the potentials $\widetilde{U}^I$ as follows

$$V(r) = \widetilde{U}^0 + (\boldsymbol{\tau}_1\cdot\boldsymbol{\tau}_2)\,\widetilde{U}^1,$$

$\boldsymbol{\tau}_{1,2}$ are the isospin Pauli matrices. The terms $V_{S,D,T}^I$ are

$$V_i^1(r) = \widetilde{U}_i^0(r) + \widetilde{U}_i^1(r)\,,\;\; V_i^0(r) = \widetilde{U}_i^0(r) - 3\widetilde{U}_i^1(r)\,,\;\; i = S, D, T\,.$$

The potentials $\widetilde{U}_i^I(r)$ consist of the real and imaginary parts:

$$\widetilde{U}_i^0(r) = \left(U_i^0 - i\,W_i^0\right)\theta\left(a_i^0 - r\right),$$
$$\widetilde{U}_i^1(r) = \left(U_i^1 - i\,W_i^1\right)\theta\left(a_i^1 - r\right) + U_i^\pi(r)\theta\left(r - a_i^1\right),$$

where $\theta(x)$ is the Heaviside function, U_i^I, W_i^I, a_i^I are free parameters fixed by fitting the experimental data, and $U_i^\pi(r)$ are the terms in the pion-exchange potential.

	$\widetilde{U}_S^0$	$\widetilde{U}_D^0$	$\widetilde{U}_T^0$	$\widetilde{U}_S^1$	$\widetilde{U}_D^1$	$\widetilde{U}_T^1$
U_i (MeV)	-458^{+10}_{-12}	-184^{+17}_{-20}	-43^{+4}_{-3}	1.9 ± 0.6	991^{+13}_{-15}	$-4.5^{+0.2}_{-0.1}$
W_i (MeV)	247 ± 5	82^{+13}_{-7}	-31^{+2}_{-6}	$-8.9^{+0.8}_{-0.5}$	5^{+14}_{-20}	$1.7^{+0.2}_{-0.1}$
a_i (fm)	$0.531^{+0.007}_{-0.006}$	$1.17^{+0.02}_{-0.03}$	0.74 ± 0.03	1.88 ± 0.02	0.479 ± 0.003	2.22 ± 0.03
g	$g_p = 0.338 \pm 0.004$			$g_n = -0.15 - 0.33i \pm 0.01$		

The parameters of the short-range potential.

The asymptotic forms of four independent regular solutions

Solutions, which have no singularities at $r=0$, at large distances are

$$\Psi^T_{1R}(r) = \frac{1}{2i}\left(S_{11}\chi^+_{p0} - \chi^-_{p0},\, S_{12}\chi^+_{p2},\, S_{13}\chi^+_{n0},\, S_{14}\chi^+_{n2}\right),$$
$$\Psi^T_{2R}(r) = \frac{1}{2i}\left(S_{21}\chi^+_{p0},\, S_{22}\chi^+_{p2} - \chi^-_{p2},\, S_{23}\chi^+_{n0},\, S_{24}\chi^+_{n2}\right),$$
$$\Psi^T_{3R}(r) = \frac{1}{2i}\left(S_{31}\chi^+_{p0},\, S_{32}\chi^+_{p2},\, S_{33}\chi^+_{n0} - \chi^-_{n0},\, S_{34}\chi^+_{n2}\right),$$
$$\Psi^T_{4R}(r) = \frac{1}{2i}\left(S_{41}\chi^+_{p0},\, S_{42}\chi^+_{p2},\, S_{43}\chi^+_{n0},\, S_{44}\chi^+_{n2} - \chi^-_{n2}\right).$$

Here S_{ij} are some functions of the energy and

$$\chi^\pm_{pl} = \frac{1}{k_p r}\exp\left[\,\pm i\left(k_p r - l\pi/2 + \eta\ln(2k_p r) + \sigma_l\right)\right],$$
$$\chi^\pm_{nl} = \frac{1}{k_n r}\exp\left[\,\pm i\left(k_n r - l\pi/2\right)\right],$$
$$\sigma_l = \frac{i}{2}\ln\frac{\Gamma(1+l+i\eta)}{\Gamma(1+l-i\eta)}, \qquad \eta = \frac{m_p\alpha}{2k_p},$$

where $\Gamma(x)$ is the Euler Γ function.

The amplitude of $e^+e^- \to N\bar{N}$ near the threshold

In the non-relativistic approximation the amplitudes in units $\pi\alpha/\mu^2$ are

$$
\begin{aligned}
T^{p\bar{p}}_{\lambda'\lambda} &= \sqrt{2}\left[g_p u^p_{1R}(0) + g_n u^n_{1R}(0)\right](\boldsymbol{e}_{\lambda'}\cdot\boldsymbol{\epsilon}^*_\lambda) \\
&+ \left[g_p u^p_{2R}(0) + g_n u^n_{2R}(0)\right]\left[(\boldsymbol{e}_{\lambda'}\cdot\boldsymbol{\epsilon}^*_\lambda) - 3(\hat{\boldsymbol{k}}\cdot\boldsymbol{e}_{\lambda'})(\hat{\boldsymbol{k}}\cdot\boldsymbol{\epsilon}^*_\lambda)\right], \\
T^{n\bar{n}}_{\lambda'\lambda} &= \sqrt{2}\left[g_p u^p_{3R}(0) + g_n u^n_{3R}(0)\right](\boldsymbol{e}_{\lambda'}\cdot\boldsymbol{\epsilon}^*_\lambda) \\
&+ \left[g_p u^p_{4R}(0) + g_n u^n_{4R}(0)\right]\left[(\boldsymbol{e}_{\lambda'}\cdot\boldsymbol{\epsilon}^*_\lambda) - 3(\hat{\boldsymbol{k}}\cdot\boldsymbol{e}_{\lambda'})(\hat{\boldsymbol{k}}\cdot\boldsymbol{\epsilon}^*_\lambda)\right],
\end{aligned}
$$

where $\boldsymbol{e}_{\lambda'}$ is a virtual photon polarization vector, corresponding to the spin projection $J_z = \lambda' = \pm 1$, $\boldsymbol{\epsilon}_\lambda$ is the spin-1 function of $N\bar{N}$ pair, $\lambda = \pm 1, 0$ is the spin projection on the nucleon momentum $\boldsymbol{k}$, and $\hat{\boldsymbol{k}} = \boldsymbol{k}/k$. The quantities $u^p_{iR}(r)$ and $u^n_{iR}(r)$ denote the first and third components of the regular solutions $\Psi_{iR}(r)$. The amplitudes g_p and g_n can be considered as the energy independent parameters.

In the non-relativistic approximation the standard formula for the differential cross section of $N\bar{N}$ pair production in e^+e^- annihilation reads

$$\frac{d\sigma^N}{d\Omega} = \frac{k_N \alpha^2}{16\mu^3}\left[\left|G_M^N(E)\right|^2\left(1+\cos^2\theta\right) + \left|G_E^N(E)\right|^2 \sin^2\theta\right].$$

Here θ is the angle between the electron (positron) momentum and the momentum of the final particle. The proton and neutron Sachs form factors are:

$$G_M^p = g_p u_{1R}^p(0) + g_n u_{1R}^n(0) + \frac{1}{\sqrt{2}}\left[g_p u_{2R}^p(0) + g_n u_{2R}^n(0)\right],$$

$$G_E^p = g_p u_{1R}^p(0) + g_n u_{1R}^n(0) - \sqrt{2}\left[g_p u_{2R}^p(0) + g_n u_{2R}^n(0)\right],$$

$$G_M^n = g_p u_{3R}^p(0) + g_n u_{3R}^n(0) + \frac{1}{\sqrt{2}}\left[g_p u_{4R}^p(0) + g_n u_{4R}^n(0)\right],$$

$$G_E^n = g_p u_{3R}^p(0) + g_n u_{3R}^n(0) - \sqrt{2}\left[g_p u_{4R}^p(0) + g_n u_{4R}^n(0)\right].$$

The elastic $N\bar{N}$ pair production cross section.

The integrated cross sections of the nucleon-antinucleon pair production have the form

$$\sigma_{\rm el}^{p} = \frac{\pi k_p \alpha^2}{4\mu^3}\left[\left|g_p u^p_{1R}(0) + g_n u^n_{1R}(0)\right|^2 + \left|g_p u^p_{2R}(0) + g_n u^n_{2R}(0)\right|^2\right],$$

$$\sigma_{\rm el}^{n} = \frac{\pi k_n \alpha^2}{4\mu^3}\left[\left|g_p u^p_{3R}(0) + g_n u^n_{3R}(0)\right|^2 + \left|g_p u^p_{4R}(0) + g_n u^n_{4R}(0)\right|^2\right]. \tag{1}$$

The label “el” indicates that the process is elastic, i.e., a virtual $N\bar{N}$ pair transfers to a real pair in a final state.

The inelastic cross section $\sigma_{\rm in}$.

There is also an inelastic process when a virtual $N\bar{N}$ pair transfers into mesons in a final state. The total cross section $\sigma_{\rm tot}$, is

$$\sigma_{\rm tot} = \sigma^{p}_{\rm el} + \sigma^{n}_{\rm el} + \sigma_{\rm in} \,. \qquad (2)$$

The total cross section may be expressed via the Green's function $\mathcal{D}(r,\, r'|E)$ of the wave equation

$$\sigma_{\rm tot} = \frac{\pi\alpha^2}{4\mu^3}\mathrm{Im}\Big[\mathcal{G}^{\dagger}\mathcal{D}\,(0,\, 0|E)\,\mathcal{G}\Big], \qquad \mathcal{G}^T = \big(g_p,\, 0,\, g_n,\, 0\big)\,, \qquad (3)$$

where the function $\mathcal{D}(r,\, r'|E)$ satisfies the equation

$$\Big[p_r^2 + \mu\mathcal{V} - \mathcal{K}^2\Big]\,\mathcal{D}\,\big(r,\, r'|E\big) = \frac{1}{rr'}\delta\,\big(r - r'\big)\ . \qquad (4)$$

The function $\mathcal{D}\,(r,\, 0|E)$ can be written as

$$\mathcal{D}\,(r,\, 0|E) = k_p \left[\Psi_{1N}(r)\Psi^T_{1R}(0) + \Psi_{2N}(r)\Psi^T_{2R}(0)\right] + k_n \left[\Psi_{3N}(r)\Psi^T_{3R}(0) + \Psi_{4N}(r)\Psi^T_{4R}(0)\right],$$

Non-regular solutions are defined by their asymptotic behavior at large distances:

$$u^p_{1N}(r) = \chi^+_{p0}\,, \;\; w^p_{2N}(r) = \chi^+_{p2}\,, \;\; u^n_{3N}(r) = \chi^+_{n0}\,, \;\; w^n_{4N}(r) = \chi^+_{n2}\,. \tag{5}$$

All other elements ψ_i of the non-regular solutions satisfy the relation

$$\lim_{r\to\infty} r\psi_i(r) = 0\,.$$

Results.

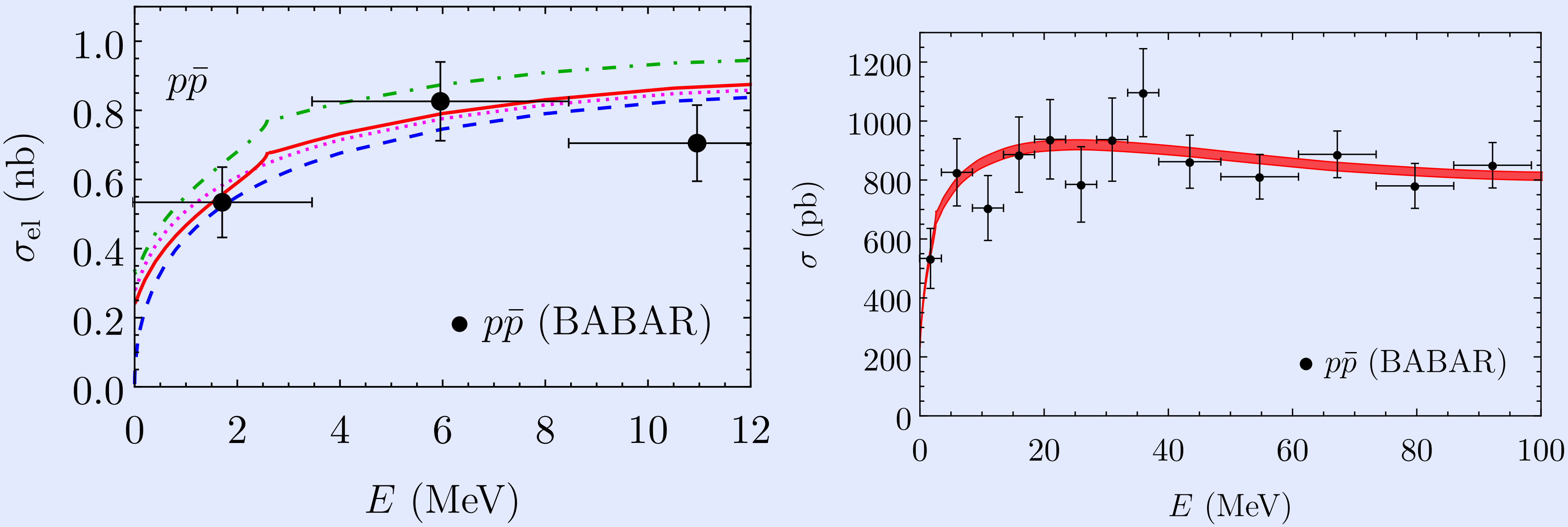

Comparison of our predictions with the data for σ_{el} of $e^+e^- \to p\bar{p}$ The experimental data are from J.P.Lees et al., BaBar, Phys.Rev. D 87, 092005 (2013).

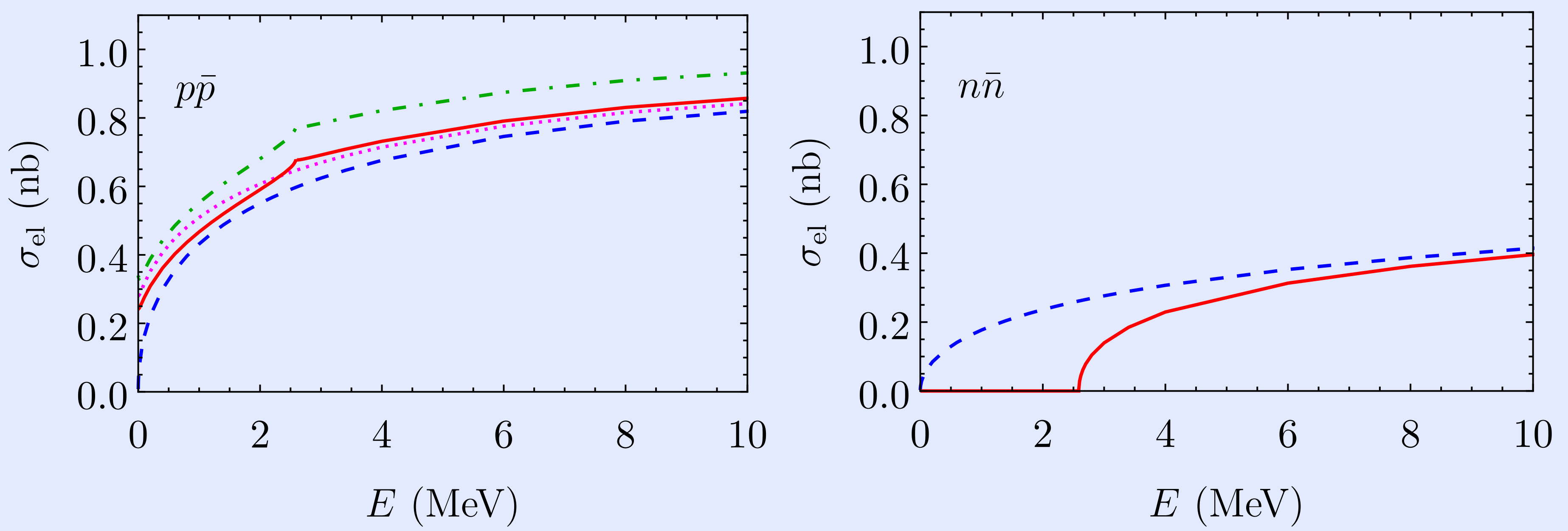

σ_{el} for $p\bar{p}$ (left) and $n\bar{n}$ (right) as a function of E of a pair. Solid curves are the exact results, dashed curves are obtained at $\Delta = 0$ and without account for the Coulomb potential, dotted curve in the left picture is obtained at $\Delta = 0$ and with account for the Coulomb potential, dash-dotted curve in the left picture corresponds to the approximation

$$\sigma_{\rm el} = C\sigma_{\rm el}^{(0)}\,, \quad C = \frac{2\pi\eta}{1 - e^{-2\pi\eta}}\,, \quad \eta = \frac{m_p\alpha}{2k_p}\,.$$

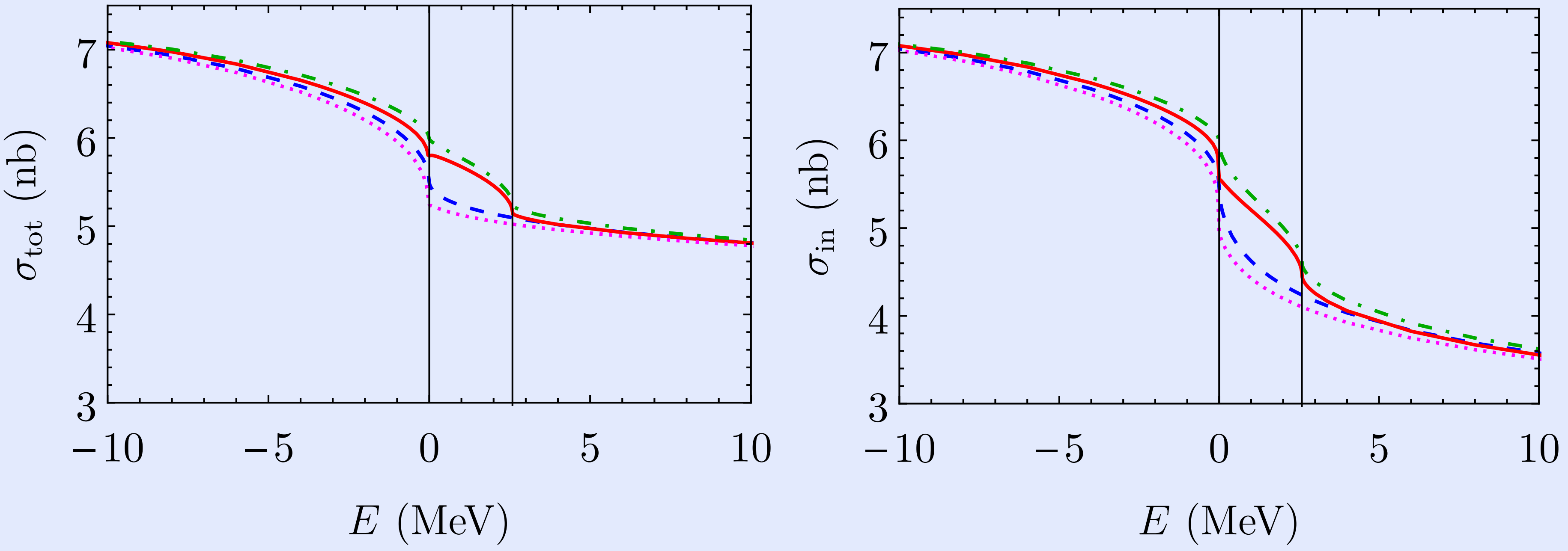

$\sigma_{\rm tot}$ (left) and $\sigma_{\rm in}$ (right) as a function of E. Solid curves correspond to the exact results, dashed curves are the results, obtained at $\Delta = 0$ and without account for the Coulomb interaction, dotted curves are obtained at $\Delta = 0$ and with account for the Coulomb potential, and dash-dotted curves are obtained at $\Delta \neq 0$ and without account for the Coulomb potential. Vertical lines show the thresholds of $p\bar{p}$ and $n\bar{n}$ pair production.

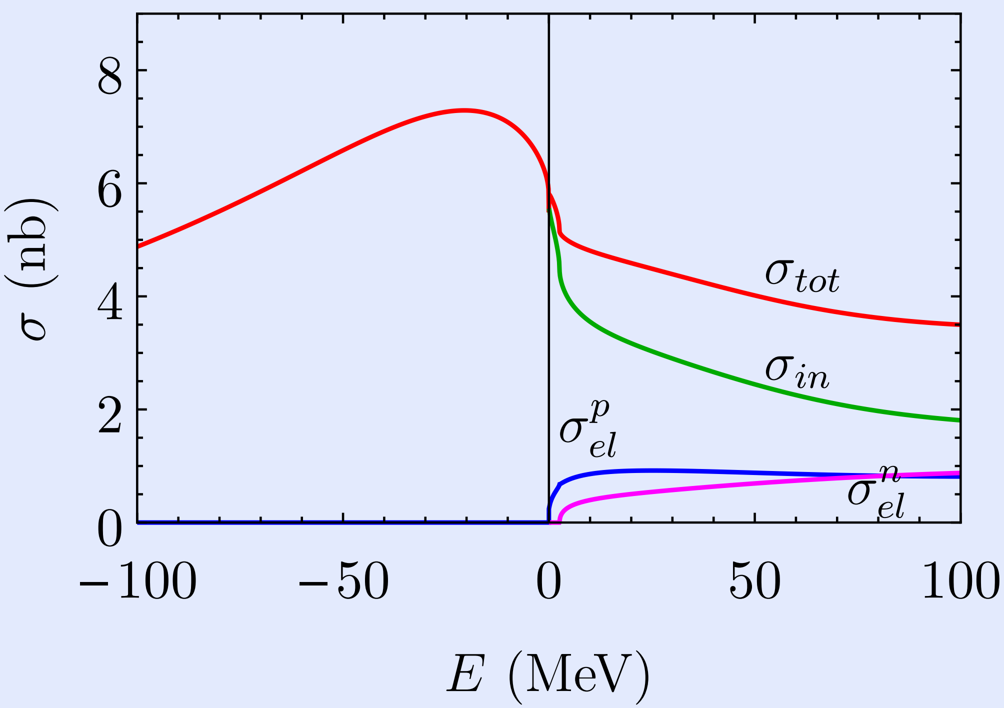

The cross sections σ_{tot}, σ_{in}, σ^p_{el}, and σ^n_{el} as a function of E.

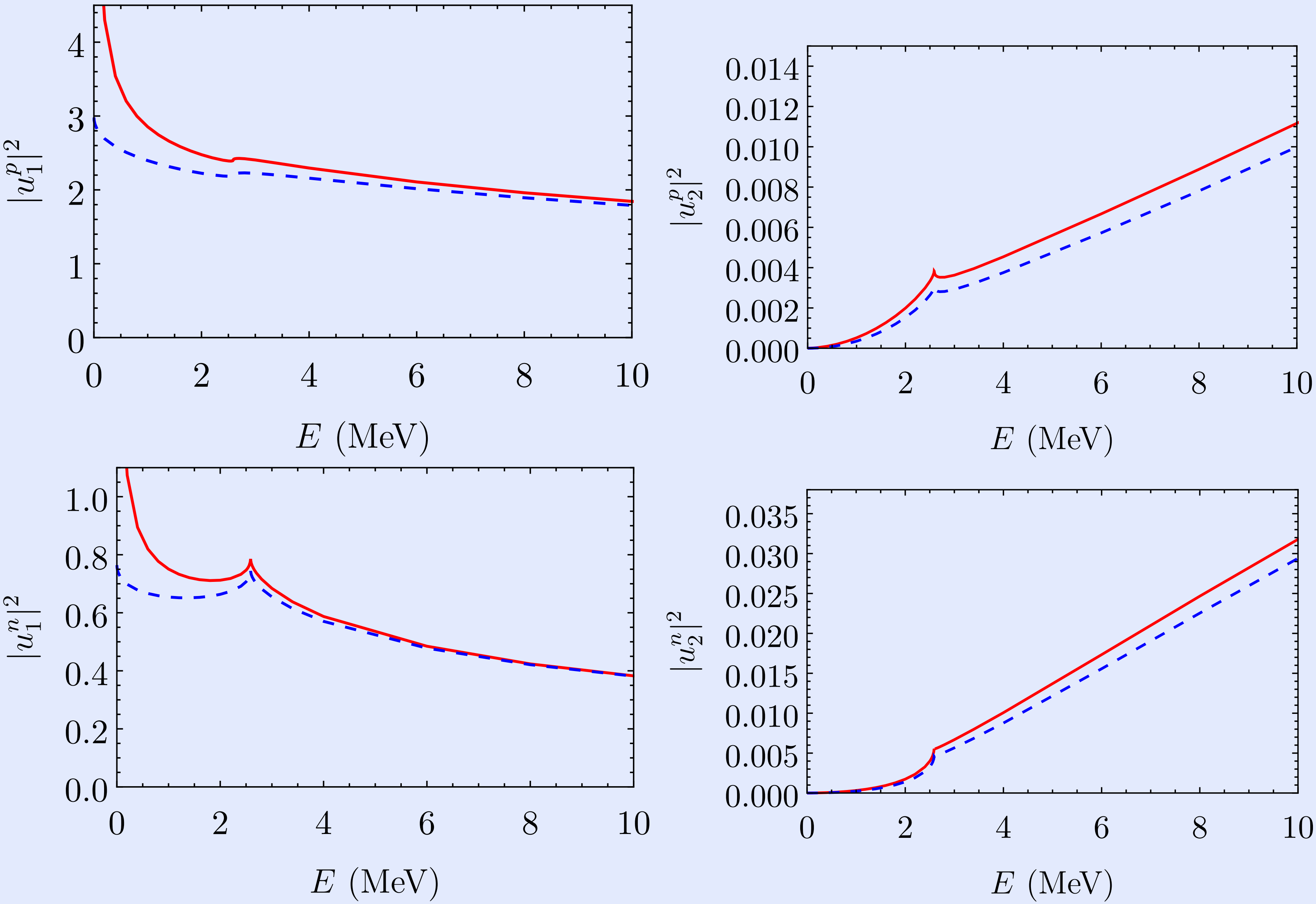

Wave functions at origin for $p\bar{p}$ in a final state. Solid curves are the exact results, dashed curves are the results, obtained without account for the Coulomb interaction.

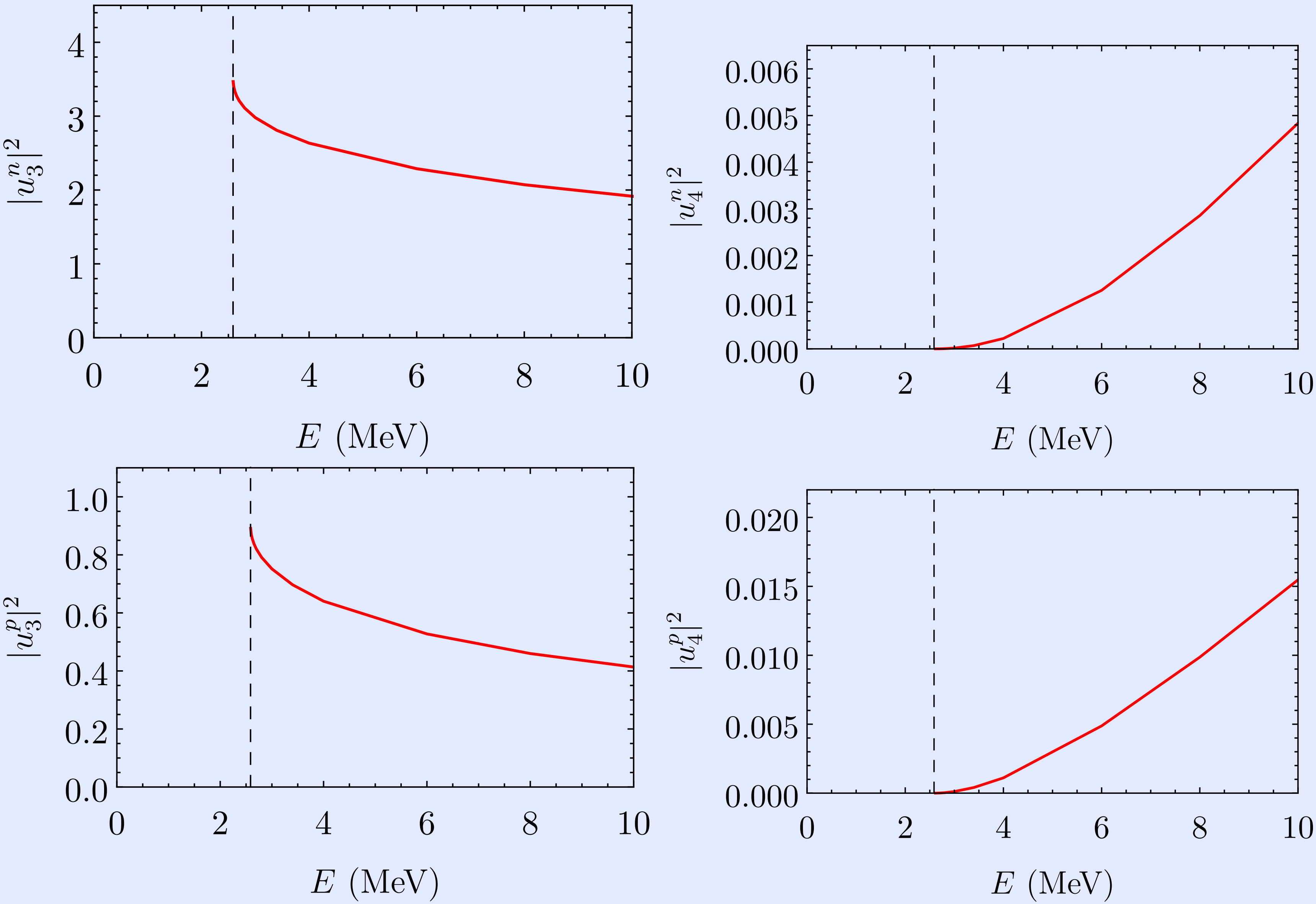

Wave functions at origin for $n\bar{n}$ in a final state. The Coulomb interaction is unimportant.

Conclusion

- We have investigated in detail the energy dependence of the cross sections of $p\bar{p}$, $n\bar{n}$, and meson production in e^+e^- annihilation in the vicinity of the $p\bar{p}$ and $n\bar{n}$ thresholds.
- Unusual phenomena are related to the interaction at large distances (”nuclear physics” of elementary particles).
- An importance of the isospin-violating effects (proton-neutron mass difference and the Coulomb interaction) is elucidated.
- Commonly accepted factorization approach for the account of the Coulomb potential does not work well enough in the vicinity of the thresholds.
- The results of SND and CMD-3 obtained at e^+e^- collider VEPP-2000 will give an important contribution to understanding of the phenomena.